

# New Phenolic Compounds Formed by Evolution of (+)-Catechin and Glyoxylic Acid in Hydroalcoholic Solution and Their Implication in Color Changes of Grape-Derived Foods

Nour-Eddine Es-Safi,\* Christine Le Guernevé, Véronique Cheynier, and Michel Moutounet

ISVV-INRA Institut des Produits de la Vigne, Unité de Recherche Biopolymères et Arômes, 2 place Viala, 34060 Montpellier, France

The reaction between (+)-catechin and glyoxylic acid in model solution system was investigated by LC/DAD and LC/ESI-MS analyses. The formation of phenolic compounds exhibiting absorption maxima near 300 nm and presenting a shoulder around 350 nm was observed. Their structures consisted of a (+)-catechin unit with one or two aldehyde groups linked at positions 6, 8 or 6 and 8 of the A ring. In addition, new yellow pigments exhibiting UV–visible spectra similar to those of xanthylum salts with absorption maxima at 450 and 280 nm were also detected. The major yellow compound was isolated and identified by ESI-MS and 1D and 2D NMR spectroscopy. The implication of these compounds in color change and browning observed during aging of grape-derived beverages is also discussed.

**Keywords:** (+)-Catechin; glyoxylic acid; model solution; browning; xanthylum salts; LC/DAD; LC/ESI-MS; NMR

## INTRODUCTION

Oxidative browning is considered to be one of the major causes of quality loss in most fruits, vegetables, and fruit-derived foods and beverages. It results in discoloration or browning after mechanical or physiological injury suffered during harvesting or storage, and this reactivity raises an important economic question.

Oxidation of polyphenols is considered to be the major browning process involving either enzymatic or nonenzymatic reactions. Enzymatic oxidation was shown to generate quinones, which are extremely reactive and take part in a complex polymerization process leading to the formation of brown pigments (Pierpoint, 1966; Simpson, 1982; Singleton et al., 1985, 1987; Gunata et al., 1987; Cillier and Singleton, 1989; Cheynier et al., 1989, 1990a,b, 1995).

Enzymatic browning usually begins when the cellular compartmentalization is disrupted, and it is generally agreed that polyphenol oxidase (PPO) is the enzyme mainly responsible for browning (Cheynier et al., 1989, 1990a; Gunata et al., 1987).

After conditioning and during storage, PPO activity decreases, and the observed browning is mainly related to nonenzymatic oxidation. In fact, it is attributed to the chemical reactions involving phenolic and nonphenolic compounds which were shown to be activated by metals especially iron (Cillier and Singleton, 1989).

It appears thus that fruit-derived foods are generally complex mixtures able to undergo, during storage, many different reactions that lead to the formation of brown polymers. The full characterization of these reactions

has not been achieved because of difficulties involved in extracting and separating the brown pigments directly from food products. Model solutions mimicking food products constitute then a simplified medium for their exploration, allowing the detection of the newly formed compounds, their isolation, and their structure elucidation.

In a previous work the enzymatic oxidation of (+)-catechin was shown to produce biaryl and biaryl ether dimer adducts (Guyot et al., 1996). These compounds were also obtained by autoxidation of (+)-catechin, and browning of white wine was shown to increase with flavanol contents (Simpson, 1982; Cheynier et al., 1989). In white-wine-like model solution containing (+)-catechin, tartaric acid, and iron ions, other colorless and yellowish compounds were obtained in addition to those formed by enzymatic reaction, which were present in trace amounts (Oszmianski et al., 1996). Further studies demonstrated that the structure of the colorless compounds consisted of oligomeric bridged compounds where flavanol units were linked by carboxymethine groups (Fulcrand et al., 1997; Es-Safi et al., 2000a). These compounds were shown to result from the reaction between (+)-catechin and glyoxylic acid obtained by oxidation of tartaric acid (Fulcrand et al., 1997). The yellow compounds were recently identified as esterified and nonesterified xanthylum salts arising from dehydration and oxidation of the colorless dimers with absorption maxima at 460 and 440 nm, respectively (Es-Safi et al., 1999a,b, 2000a).

This work describes the detection and isolation of new phenolic compounds formed by interaction between (+)-catechin and glyoxylic acid in hydroalcoholic medium. Their characterization by ESI-MS and 1D and 2D NMR techniques is also presented.

\* Address correspondence to this author at the École Normale Supérieure, Laboratoire de Chimie Organique et d'Études Physico-Chimique, B.P. 5118, Takaddoum Rabat, Morocco [fax (212) 7 750047].

## MATERIALS AND METHODS

**Reagents.** Deionized water was purified with a Milli-Q water system prior to use. Acetonitrile was purchased from BDH. Methanol, formic acid, and acetic acid were obtained from Prolabo (Fontenay S/Bois, France). (+)-Catechin was purchased from Sigma. Glyoxylic acid was from Aldrich and sodium tetraborohydride from Interchim.

**Reactions.** Reaction of (+)-catechin (**1**, 11.9 mg) in the aqueous potassium hydrogen tartrate solution or with glyoxylic acid (19.0 mg) was conducted at 39 °C in hydroalcoholic medium as described elsewhere (Oszmianski et al., 1996; Fulcrand et al., 1997; Es-Safi et al., 1999b). Reduction of compound **4a** with sodium borohydride in ethanol was performed as previously reported (Es-Safi et al., 1999b).

**Analytical HPLC/DAD analyses.** HPLC/DAD analyses were performed by means of a Waters 2690 separation module system including a solvent and a sample management system, a Waters 996 photodiode array detector, and Millennium 32 chromatography manager software. UV-visible spectra were recorded from 250 to 600 nm. The column was a reversed-phase Lichrospher 100-RP18 (5  $\mu$ m packing, 250  $\times$  4 mm i.d.) protected with a guard column of the same material. Elution conditions were as follows: 1 mL/min flow rate; temperature, 30 °C; solvent A, water/formic acid (98:2, v/v); solvent B, acetonitrile/water/formic acid (80:18:2, v/v); elution from 5 to 30% B in 40 min, from 30 to 40% B in 10 min, and from 40 to 100% B in 5 min, followed by washing and re-equilibrating of the column.

**Semipreparative HPLC Purification.** HPLC separations at the semipreparative scale were performed by means of a Gilson system including a 305 master and a 306 slave pump, an 806 manometric module, an 811 dynamic mixer, a 7161 Rheodyne valve injector fitted with a 2 mL sample loop, and an 875 UV-visible Jasco detector set at 280 nm. The column was a reversed-phase Microsorb C18 (5  $\mu$ m packing, 125  $\times$  22 mm i.d.). The following elution conditions were used: 7 mL/min flow rate; solvent A, water/acetic acid (99:1, v/v); solvent B, methanol/solvent A (80:20, v/v); elution from 15 to 60% B in 10 min and from 60 to 90% B in 15 min, followed by washing and re-equilibrating of the column.

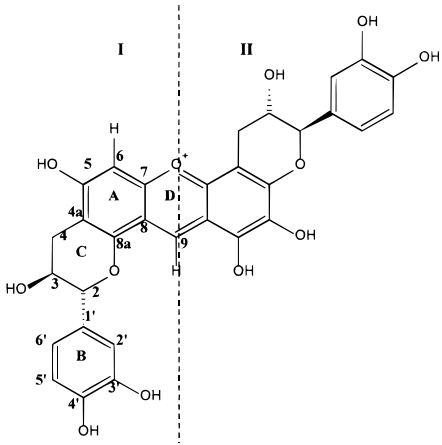
**MS Apparatus and LC/MS Analyses.** MS measurements were performed on a Sciex API I Plus simple quadrupole mass spectrometer with a mass range of 2400 amu, equipped with an electrospray ionization source. The mass spectrometer was operated in positive- and negative-ion modes. Ion spray voltage was selected at -4 kV and orifice voltage at -60 or +60 V in negative or positive mode, respectively. Elemental composition calculated for compound **4a**, C<sub>31</sub>H<sub>25</sub>O<sub>12</sub>: C, 63.16%; H, 4.27%; O, 32.57%. Found: C, 63.02%; H, 4.47%; O, 32.51%.

HPLC separations were carried out on a narrowbore reversed-phase column with an ABI 140 B solvent delivery system (Applied Biosystems, Weiterstadt, Germany). The column was connected with the ion spray interface via a fused-silica capillary (length = 100 cm, 100  $\mu$ m i.d.). The reaction mixture was injected with a rotary valve (Rheodyne model 8125) fitted with a 20  $\mu$ L sample loop. The separation was achieved on a Lichrospher 100-RP18 column (5  $\mu$ m packing, 250  $\times$  4 mm i.d.; Merck, Darmstadt, Germany), with a flow rate of 280  $\mu$ L/min. The elution was done with solvents A and B used in HPLC/DAD analysis, and the conditions were adapted as follows: isocratic 10% B in 4 min, linear gradient from 10 to 15% B in 11 min, from 15 to 50% B in 25 min, and from 50 to 100% B in 5 min, followed by washing and reconditioning of the column. The absorbance at 280 nm was monitored by an ABI 785A programmable absorbance detector and by a Waters 990 diode array detector linked to 990 system manager software.

**Absorption Spectra.** UV-visible spectra were recorded with a Kontron Uvikon 930 spectrophotometer fitted with a quartz cell. Spectra were registered in pH 2.5 acid medium, and the pH was increased to 8.5 by the addition of NaOH solution drops.

**NMR Analysis.** NMR spectra of samples (~6 mg) in [2H<sub>6</sub>]-DMSO/TFA (9:1 v/v) (250  $\mu$ L) were acquired on a Varian

**Table 1.** <sup>1</sup>H and <sup>13</sup>C Assignments of Compound **4a** in TFA/DMSO-*d*<sub>6</sub> (1:9)

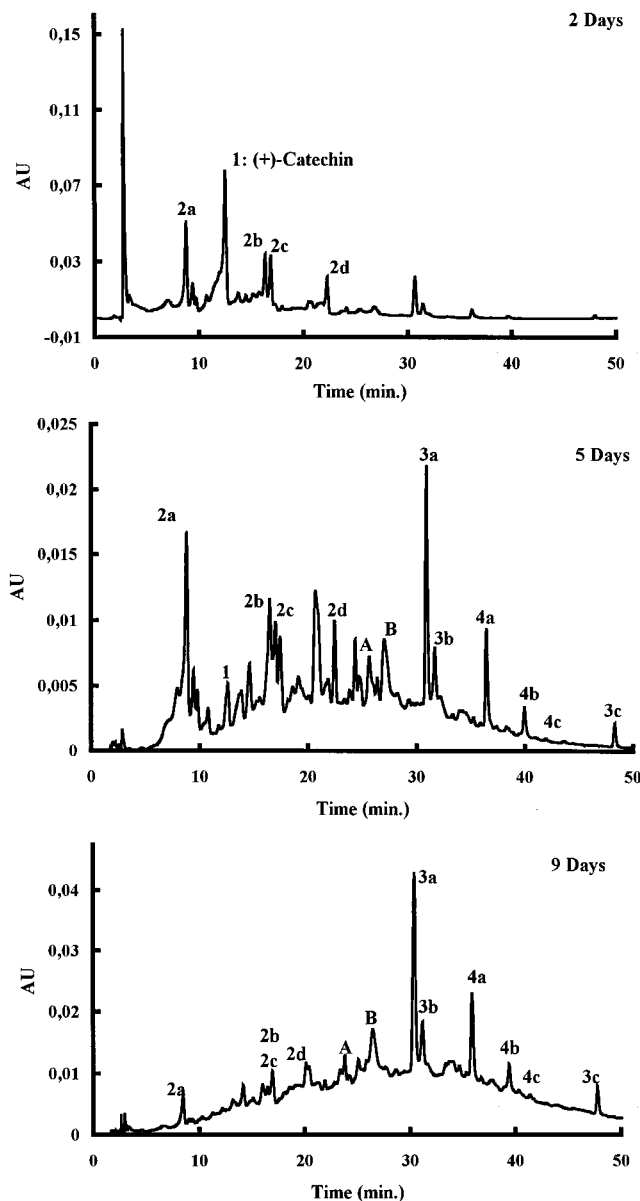


position	system I		system II	
	<sup>1</sup> H	<sup>13</sup> C	<sup>1</sup> H	<sup>13</sup> C
2	5.13 d (6.14)	82.8	5.36 d (4.6)	83.6
3	4.16 m	64.9	4.27 m	64.4
4 $\alpha$	2.64 dd (17.3; 6.2)	26.2	2.91 dd (17.3; 3.6)	24.0
4 $\beta$	2.73 dd (17.3; 4.0)	26.2	3.02 dd (17.3; 5.2)	24.0
5		171.4		148.5
6	6.93 s	94.8		nd
7		156.6		143.0
8		110.0		nd
4a		108.2		100.8
8a		154.5		157.9
1'		128.8		128.9
2'	6.72	114.1	6.75	113.5
3'		145.8		145.8
4'		145.8		145.8
5'	6.78	113.7	6.70	115.7
6'	6.61 dd (1.5; 8.2)	118.1	6.66 dd (1.5; 8.2)	117.5
9	9.39	141.5		

UNITY INOVA 500 spectrometer equipped with a 3 mm indirect detection probe operating at 500 MHz for <sup>1</sup>H and 125.7 MHz for <sup>13</sup>C and processed using FELIX (Biosym Technologies) on a Silicon Graphics workstation. The temperature was maintained at 297 K. Chemical shifts ( $\delta$ ) are given in parts per million, and coupling constant *J* values are given in hertz. The central solvent signals of DMSO were used as internal reference (<sup>1</sup>H,  $\delta$  2.5; <sup>13</sup>C,  $\delta$  39.5 relative to TMS). The <sup>1</sup>H and <sup>13</sup>C data for compound **4a** are shown in Table 1.

## RESULTS AND DISCUSSION

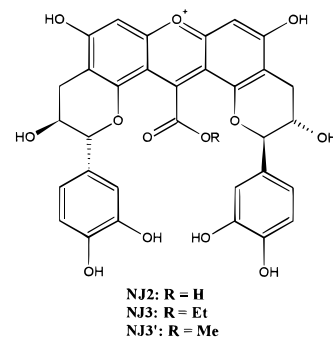
The reaction of (+)-catechin and glyoxylic acid was investigated as a model of browning phenomenon, which is generally observed during the aging of grape-derived foods. (+)-Catechin is one of the most common grape flavanols, and glyoxylic acid has been shown to be formed in model solution systems by the oxidation of tartaric acid (Fulcrand et al., 1997). In fact, the reaction was conducted first between (+)-catechin and tartaric acid in iron catalytic medium to generate a pH similar to that of wine (Oszmianski et al., 1996). In both cases, colorless and yellowish compounds were obtained. However, the complexity of the chromatographic profiles made isolation and purification of the compounds difficult to achieve when tartaric acid was used. The reaction between (+)-catechin and glyoxylic acid was thus preferred to that with tartaric acid as it is direct and gives a higher yield. The originally colorless solution of (+)-catechin and glyoxylic acid became brown with time, and the appearance of new compounds initially absent in the mixture was observed by LC/DAD analysis.



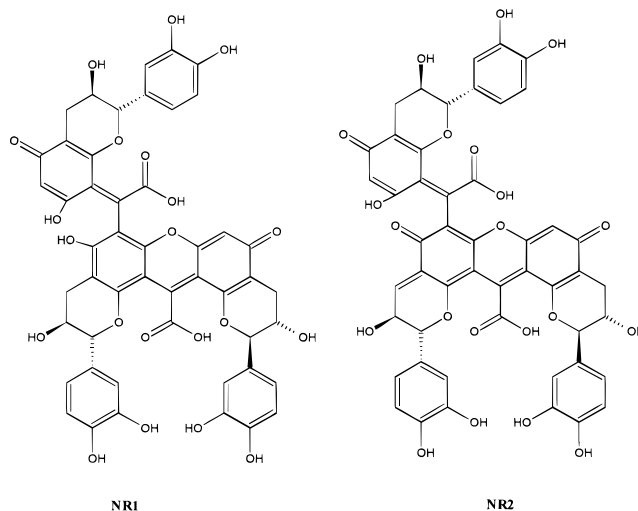
**Figure 1.** Chromatographic profiles registered at 280 nm with HPLC/DAD system and showing the evolution of a mixture containing (+)-catechin and glyoxylic acid.

Figure 1 shows chromatographic profiles recorded at 280 nm and at various stages of the reaction. A rapid decrease of (+)-catechin (**1**), concomitant with the appearance of new products initially absent in the mixture, was observed. The formed compounds proceeded later to more polymerized derivatives eluted as a bump in the chromatographic profile as shown in the chromatogram recorded after 9 days of incubation.

Among the obtained compounds, the four products **2a**, **2b**, **2c**, and **2d**, previously identified as dimeric derivatives in which two (+)-catechin units are linked to each other by carboxymethine groups via their 6 and 8 A ring tops, were detected (Fulcrand et al., 1997; Es-Safi et al., 2000a). Kinetic studies of their formation showed that they gradually accumulated at the beginning of the incubation period and then were converted to more polymerized compounds and/or other degradation products. Compound **2a**, which is the isomer having two catechin units linked through their 8 tops, is the major one formed followed by the isomers **2b** and **2c**, in which the 6 and 8 A rings are involved. Isomer **2d**, in which



**Figure 2.** Structures of the xanthylum salts (NJ2, NJ3, and NJ3'), previously identified (Es-Safi et al., 1999a,b, 2000a).



**Figure 3.** Proposed structures for compounds NR1 and NR2.

the two 6 A rings tops are involved, is the isomer formed to the lowest extent. This difference is probably due to the relatively high reactivity of the 8 top compared to that of the 6 one.

The role of these colorless compounds as intermediates in the reaction pathways leading to brown pigments has been demonstrated earlier (Es-Safi et al., 1999a–c, 2000a). Thus, xanthene compounds obtained by dehydration between the two A ring aromatic hydroxyl groups were shown to be formed from the four colorless compounds. These xanthene derivatives were further oxidized to yellow compounds with a xanthylum skeleton as previously reported (Figure 2).

The detection of new red compounds, named NR1 and NR2 and exhibiting UV–visible spectra with absorption maxima around 560, was also observed during the first 9 days of the evolution of these colorless compounds as previously reported (Es-Safi et al., 1999b,d). LC/ESI-MS analysis conducted in the negative ion mode showed signals at  $m/z$  at 959 and 957 for NR1 and NR2, respectively, indicating their trimer-based structures. On this basis, the structures shown in Figure 3 were proposed for these compounds. The presence of a quinonoidal skeleton could explain the absorption around 560 nm observed for both compounds.

In addition to the colorless compounds, **2a–d**, which have UV–visible spectra similar to that of (+)-catechin, other unreported polyphenolic compounds were observed as shown in the chromatographic profiles recorded at 300 and 450 nm after 5 days of incubation (Figure 4). Thus, in the chromatographic profile recorded at 300 nm, three compounds, **3a**, **3b**, and **3c**,

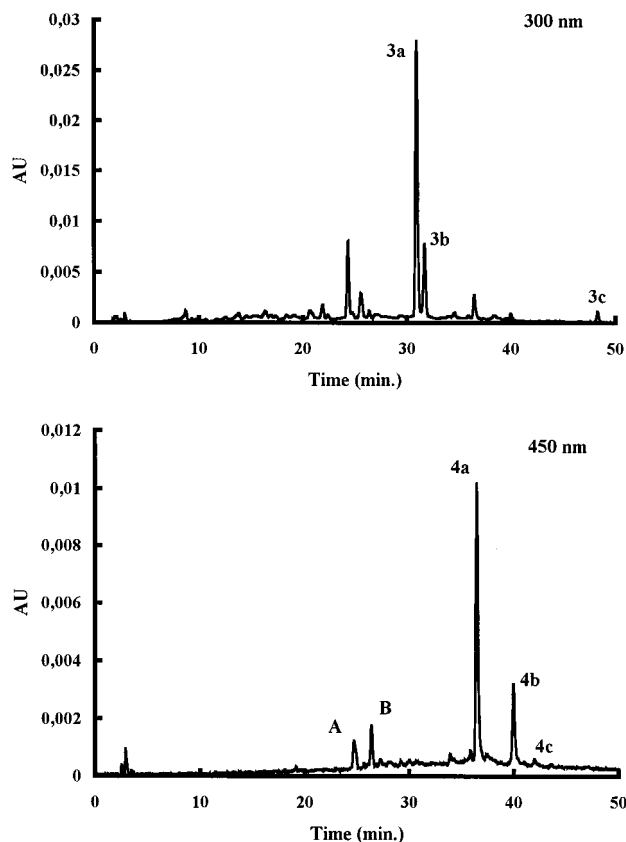


**Figure 4.** HPLC chromatograms registered at 300 and 450 nm, after 5 days of incubation and showing the newly formed phenolic compounds.

exhibiting UV-visible absorption maxima at 295 nm and a shoulder around 340 nm, were detected. In the chromatographic profile recorded at 450 nm three other new compounds, **4a**, **4b**, and **4c**, were observed. Finally, two other phenolic compounds, **A** and **B**, exhibiting UV-visible spectra similar to those of the previously reported NJ3 and NJ3' compounds (Es-Safi et al., 1999b, 2000a), with absorption maxima at 460 nm, but showing different retention times, were also detected.

LC/ESI-MS analysis conducted in the negative-ion mode showed signals at  $m/z$  317 for compounds **3a** and **3b**, at  $m/z$  345 for compound **3c**, and at  $m/z$  587 for compounds **4a**, **4b**, and **4c**. Finally, compounds **A** and **B** were characterized by a signal at  $m/z$  643 as previously reported for the xanthylum compounds NJ3 and NJ3' (Es-Safi et al., 1999b, 2000a).

Complete structural elucidation of compounds **3a**, **3b**, and **3c**, achieved by 1D and 2D NMR analyses (Es-Safi et al., 2000b), showed that they consisted of (+)-catechin units with one aldehyde group linked to position 6 or 8 of the aromatic A ring, respectively, for **3a** and **3b**, whereas both positions were substituted by aldehydic groups in compound **3c** (Figure 5).

The UV-visible spectra of the three other new phenolic compounds, **4a**, **4b**, and **4c**, were similar to those of xanthylum salts with two absorption maxima around 450 and 280 nm, respectively (Figure 6A). These maxima were bathochromically shifted to 485 and 296 nm by the addition of alkaline solution drops in agreement with the data reported on xanthylum salt derivatives (Jurd and Somers, 1970; Hrazdina and Borzell, 1971; Dangles and Brouillard, 1994; Es-Safi et al., 1999a,b). This bathochromic shift was accompanied by

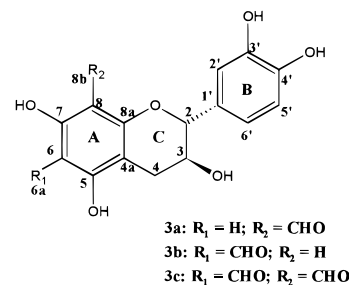


**Figure 5.** Structure of compounds **3a**, **3b**, and **3c** (Es-Safi et al., 1999f).

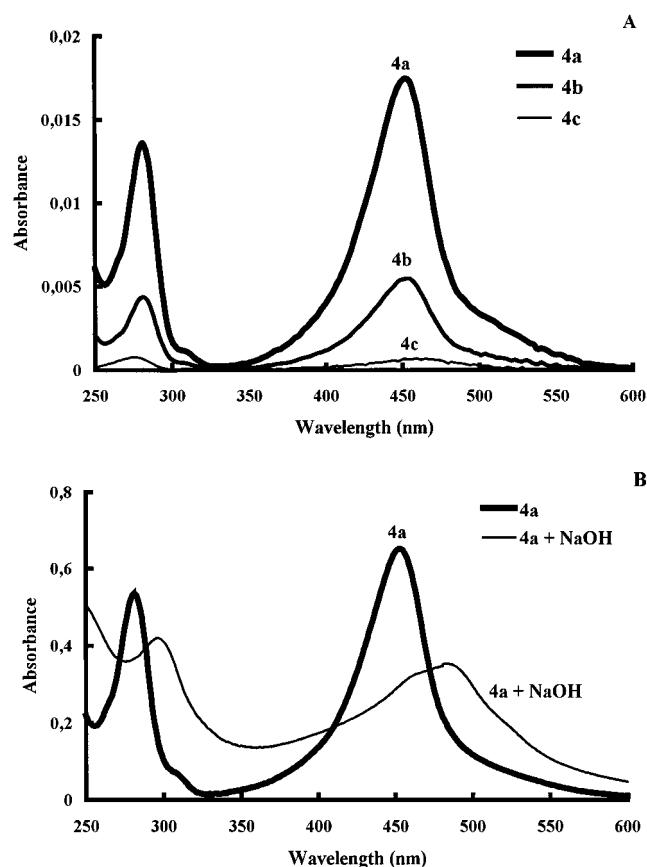


**Figure 6.** (A) UV-visible spectra of compounds **4a**, **4b**, and **4c** in acidic medium. (B) UV-visible spectra of compound **4a** in acidic and alkaline medium showing the bathochromic shift occurring by addition of sodium hydroxide drops.

a decrease of the intensity of their maximum absorption at 450 nm as shown for compound **4a** in Figure 6B.

LC/ESI-MS analysis conducted in the negative-ion mode showed similar signals at  $m/z$  587 ( $M_r = 589$ ) for compounds **4a**, **4b**, and **4c**, corresponding to  $[M - 2H]^-$  in addition to  $[M - H + HCOO]^-$  observed at  $m/z$  633 (Figure 7). Additional signals observed at  $m/z$  435 corresponded to  $[M - 2H - 152]^-$  due to the retro-Diels-Alder fission. These results indicated thus that compounds **4a**, **4b**, and **4c** differed from the previously identified xanthylum salts NJ2 and NJ3, which have molecular weights of 617 and 645, respectively (Es-Safi et al., 1999a,b). Isolation of compounds **4a-c** was then performed by HPLC at the semipreparative scale. Under the conditions described in Materials and Methods, compounds **4a**, **4b**, and **4c** were eluted, respectively, at 17, 19, and 23 min. Amorphous brownish powders of these compounds were finally obtained after concentration under vacuum, freezing, and lyophilization. Com-

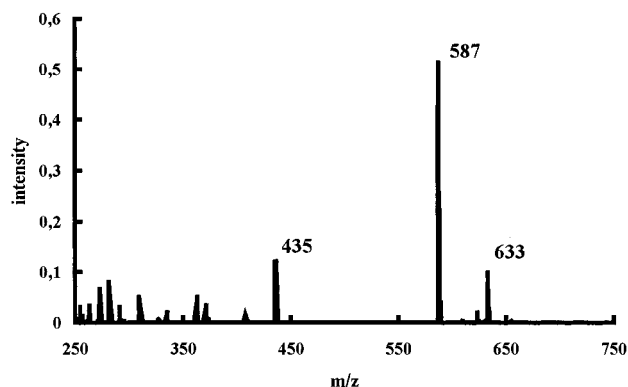


**Figure 7.** Mass spectrum of compounds **4a** ( $m/z$  587).

pound **4a** was obtained in sufficient amounts (10 mg) to allow its structure investigation.

The reduction of compound **4a** was performed by sodium tetraborohydride in alcoholic solution medium and was followed by LC/DAD and LC/ESI-MS analysis. Disappearance of the yellowish coloration of compound **4a** concomitant with the formation of a new compound exhibiting absorption maximum at 280 was observed. Through LC/ESI-MS analysis conducted in the negative-ion mode, this compound was characterized by a signal at  $m/z$  589 in agreement with its xanthene-based skeleton. The structural elucidation of compound **4a** was further achieved by 1D and 2D NMR analyses and allowed the assignment of the chemical shifts shown in Table 1 and the proposition of the accompanied structure.

In the  $^1\text{H}$  NMR spectrum, two C ring catechin systems were observed, indicating that the structure of compound **4a** was based on two catechin units. Thus, the usual pyran ring protons were assigned by  $^1\text{H}$  and HSQC experiments. The two double doublets located, respectively, at 2.64/2.73 ppm and 2.91/3.02 ppm were assigned to the H-4 $\alpha$  and H-4 $\beta$  of the two catechin systems. The two doublets located at 5.13 and 5.36 ppm were easily attributed to the C ring H-2 protons due to their chemical shifts and their correlations in HSQC experiment with the two signals located at 82.8 and 83.6 ppm, respectively, corresponding to the oxygenated aliphatic carbons C-2. Finally, the two multiplets located at 4.16 and 4.27 ppm were assigned to the two H-3 protons.

In the aromatic region the two H-6' protons were observed as two double doublets, respectively, at 6.61 and 6.66 ppm, and the two H-2' and H-5' were observed as multiplets between 6.70 and 6.80 ppm. In the aromatic A ring region, only one proton signal appearing as a singlet located at 6.93 ppm was present, and finally a more deshielded singlet at 9.39 ppm was also observed.

These results showed that compound **4a** was a xanthylum salt derivative containing two (+)-catechin units in which three of the four 6 and 8 positions are substituted, because only one proton signal was observed by NMR analysis. The more deblinded proton was attributed to the H-9 proton of the pyrylium D ring. Its observed chemical shift (9.39 ppm) is in agreement with its chemical environment in addition to its correlation in HSQC experiment with a carbon located at 141.5 ppm and corresponding to the C-9.

Upon HMBC experiment analysis, the proton signals located, respectively, at 5.13, 4.16, 2.64, and 2.73 ppm were attributed to H-2, H-3, and two H-4 of the same

catechin spin system (named I), whereas those located at 5.36, 4.27, 2.91, and 3.02 ppm were attributed to those of the other catechin spin system (named II).

In addition to their long-range correlation with the heterocyclic C ring carbons, the H-4 protons of system I correlated with the signal carbons located at 108.2, 154.5, and 171.4 ppm. The signal located at 154.5 ppm was attributed to the C-8a carbon due to its correlation with the H-2 proton via the oxygen atom, and that located at 108.2 ppm was attributed to the C-4a carbon due to its chemical shift and its correlation with the H-3 proton. Finally, the signal located at 171.4 ppm was then attributed to the hydroxylated aromatic C-5 carbon. The C-5 and C-4a attributed above showed correlations with the residual A aromatic proton located at 6.93 ppm, indicating its belonging to this catechin system. Because the 8 proton could not show an intense correlation with C-5, the singlet located at 6.93 ppm was then attributed to H-6. In addition, this residual aromatic proton showed correlations with two carbons located at 110.0 and 156.6 ppm. The latter was attributed to the C-7 due to its chemical shift, whereas the former was assigned to C-8. This was further confirmed by the presence of a correlation between the H-9 proton (9.39 ppm) and the C-8a carbon located at 154.5 ppm, indicating the substitution of the CH group in the 8 position of the catechin I spin system.

It must also be noted that the chemical shifts of the catechin spin system I were similar to those of the previously reported xanthylum salt derivative NJ2 (Es-Safi et al., 1999a) in agreement with the proposed structure.

In the catechin II spin system the H-2 proton was easily attributed to the doublet located at 5.36 ppm as previously indicated. In addition to its long-range correlation with the C-3 (64.4 ppm), C-4 (24.0 ppm), C-2' (113.5 ppm), C-6' (117.5 ppm), and C-1' (128.8 ppm) carbons, this proton showed a correlation with a signal located at 157.9 ppm, which correspond to the chemical shift of an aromatic carbon linked to an oxygen atom like the C-5, C-7, or C-8a carbon. The latter is in a favorable position to show such correlation via the oxygen atom of the pyran C ring, and thus the signal at 157.9 was attributed to the C-8a carbon.

The two H-4 protons of this catechin system were attributed to the signals located at 2.91 and 3.02 ppm from the HSQC experiment. In the HMBC spectrum, they showed correlations with the pyranic C ring C-2 and C-3 carbons located, respectively, at 83.6 and 64.4 ppm. In addition, they showed correlations with carbon signals located at 100.8, 148.5, and 157.9 ppm, the latter being attributed to the C-8a. The two remaining signals were attributed to C-4a and C-5 due to their chemical shift, the latter being in agreement with a hydroxylated aromatic carbon. The C-5 carbon thus identified showed a correlation with the H-9 proton, showing thus that the C-9 carbon is linked to the 6-position because the 8-position linkage could not allow such correlation. Another correlation between H-9 and a signal located at 143.0 ppm and attributed to the C-7 carbon was also shown. The obtained results allowed thus assignment of hydrogen and carbon atom chemical shifts shown in Table 1.

These results showed thus that the catechin I system involved its 7- and 8-positions in the pyrylium D ring (Figure 8). The 8-position is linked to the C-6 of system II via the pyrylium C-9 carbon, and the 7-position is

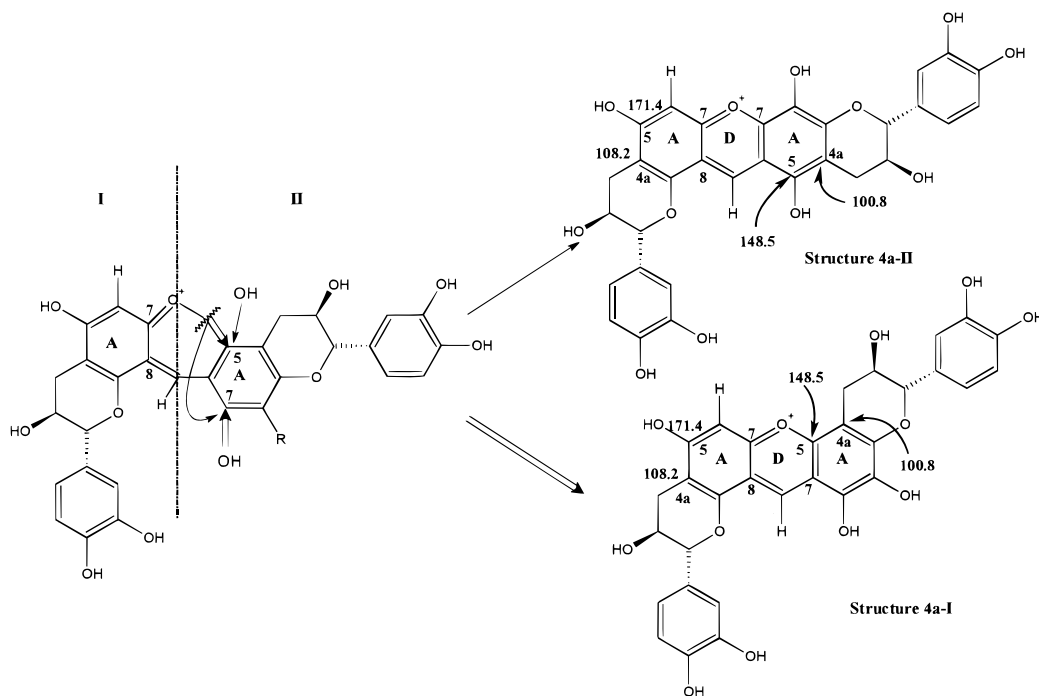


**Figure 8.** Two hypothetical structures of compound **4a**.

linked to the oxygen D ring. As shown in Figure 8, both the 5- and 7-positions of system II could be considered as linkage sites to form the xanthylum D ring. These two possibilities give thus the two structures **4a-I** and **4a-II** proposed for compound **4a**. The R group linked to the 8-position of the catechin system II was determined on the basis of ESI-MS analysis. Because the molecular weight of compound **4a** is 589, the R group must have a molecular weight of 17 amu. An additional hydroxyl group was thus suggested to be linked to the disubstituted A ring catechin system, giving a compound with  $C_{31}H_{25}O_{12}$  as its empirical formula. This is in agreement with the obtained NMR data, where neither additional carbon nor protons were observed, and with the elemental composition determined by high-resolution mass spectroscopy.

Examination of the carbon chemical shifts showed that those of the two C-4a and C-5 carbons of catechin spin system I (108.2 and 171.4 ppm), which were similar to those reported for compound NJ2 (Es-Safi et al., 1999a), differed from those of system II (100.8 and 148.5 ppm). This showed that they must have different chemical environments such as those presented in the **4a-I** structure, because those of the **4a-II** structure seemed to be too similar to explain such chemical shift differences. The less deblinded position of the C-4a and C-5 carbons of catechin spin II system could be explained by the proximity of the positive charge of the xanthylum D ring. Moreover, the C-5 carbon is directly linked to the positively charged oxygen of the pyrilium D ring.

In addition, examination of the two structures showed that only **4a-I** contained an ortho-dihydroxyl group on the xanthylum skeleton. Its presence was confirmed by UV-visible spectroscopy through aluminum chloride complexation. As indicated, compound **4a** exhibited UV-visible spectrum similar to that of xanthylum salt derivatives with two absorption maxima at 280 and 450 nm, respectively. These maxima were bathochromically shifted by increasing the pH in agreement with the data reported on xanthylum salts (Jurd and Somers, 1970;

Hrazdina and Borzell, 1971; Dangles and Brouillard, 1994). This was also accompanied by a decrease of intensity probably due to the presence of sensitive hydroxyl groups as reported for some flavonols (Jurd and Horowitz, 1957; Mabry et al., 1970).

When the spectrum was recorded in neutral pH medium, a slight bathochromic shift and a decrease in the intensity of the absorption maximum at 450 nm were observed. This is due to the passage from the xanthylum-based skeleton to the neutral quinonoidal form as previously reported for hydroxyxanthylum salt derivatives (Dangles and Brouillard, 1994). When aluminum chloride was added, an irreversible bathochromic shift of the absorption maxima, which was then located at 482 nm, was observed, indicating the formation of the aluminum complex. The irreversibility of the bathochromic shift with pH decrease is due to the fact that the aluminum complex occurred between the hydroxyl and carbonyl groups as shown in Figure 9. This complex was demonstrated to be insensitive to the pH effects (Jurd, 1962; Mabry et al., 1970), in agreement with the results obtained with compound **4a**. These results showed thus that the structure of compound **4a** was then **4a-I**.

From a mechanistic point of view, the xanthylum **4a** formation could be envisaged from the previously identified compounds **3a** as shown in Figure 10. In acidic pH medium, compound **3a** yielded the dimer **5** according to a mechanism similar to that shown with acetaldehyde and glyoxylic acid (Timberlake and Bridle, 1976; Fulcrand et al., 1997). The intramolecular dehydration or substitution of this dimer followed by an oxidation process gives, respectively, the xanthenes **6** and **7**. The transformation of the latter to the *o*-dihydroxyxanthene derivative **8** could be obtained by loss of a formic acid molecule. Further acid-catalyzed dehydration of compound **8** gives finally the xanthylum salt derivative **4a**.

In addition to the xanthylum **4a**, the formation of xanthylum salt **11** could also be envisaged from the xanthene **6**, which yields the xanthene derivative **9** by oxidation. Further esterification of compound **9** followed

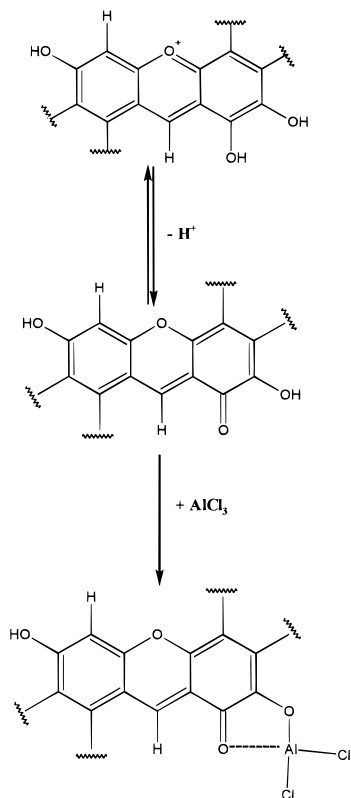


**Figure 9.** Hypothetical structural transformations and aluminum chloride effect on compound **4a**.

by an acid-catalyzed dehydration process gives the esterified xanthylum **11**. The formation of the latter explained the detection by LC/DAD of compounds **A** and **B** with maximum absorption at 460 nm as that previously reported for the esterified xanthylum salt NJ3 (Es-Safi et al., 1999b, 2000a). This was also confirmed by LC/MS analysis conducted in the negative-ion mode, which showed signals at  $m/z$  643 in agreement with the basic xanthylum **11** structure.

## CONCLUSION

This study showed the major role played by tartaric acid and glyoxylic acid in the condensation of flavanols giving various colorless and colored polyphenolic compounds. The formation of such compounds in a model solution system indicates their probable contribution in color transformation of fruit-derived foods (Somers, 1971; Haslam, 1980). In addition, the presence of an aldehyde moiety in the structure of some of the detected compounds allowed them to play a role of polymerizing agent such as that observed in the case of acetaldehyde or glyoxylic acid (Fulcrand et al., 1997). This explains the ability of such a solution to give more highly polymerized compounds that finally precipitate. The identification of new xanthylum salt derivatives in addition to those previously identified showed the structural variability of these compounds and constitutes a new support for their contribution in color change and browning as previously postulated (Somers, 1971). The proposed structures of compounds NR1 and NR2 are a new support for the implication of xanthylum salt derivatives in the formation of more polymeric colored compounds and the contribution of quinonoidal derivatives on the color change of grape-derived foods as previously postulated (Somers, 1971).

The formation in grape-derived foods of products formed under the experimental conditions assayed is very likely. However, the formation of such products proceeds very quickly in the experiment described in this paper compared to those probably formed in fruit-derived foods, which may be relatively slow during conservation and aging. Nevertheless, it is expected that such an experiment may at least enable elucidation of the simpler polymerization products such as those slowly formed during maturation and storage. Their yellowish color may to an extent explain the apparent similarity that a very old white wine or a very old red wine, under certain conditions, attains. In particular, the absorption maxima of the newly detected xanthylum derivatives matched well the absorption increase

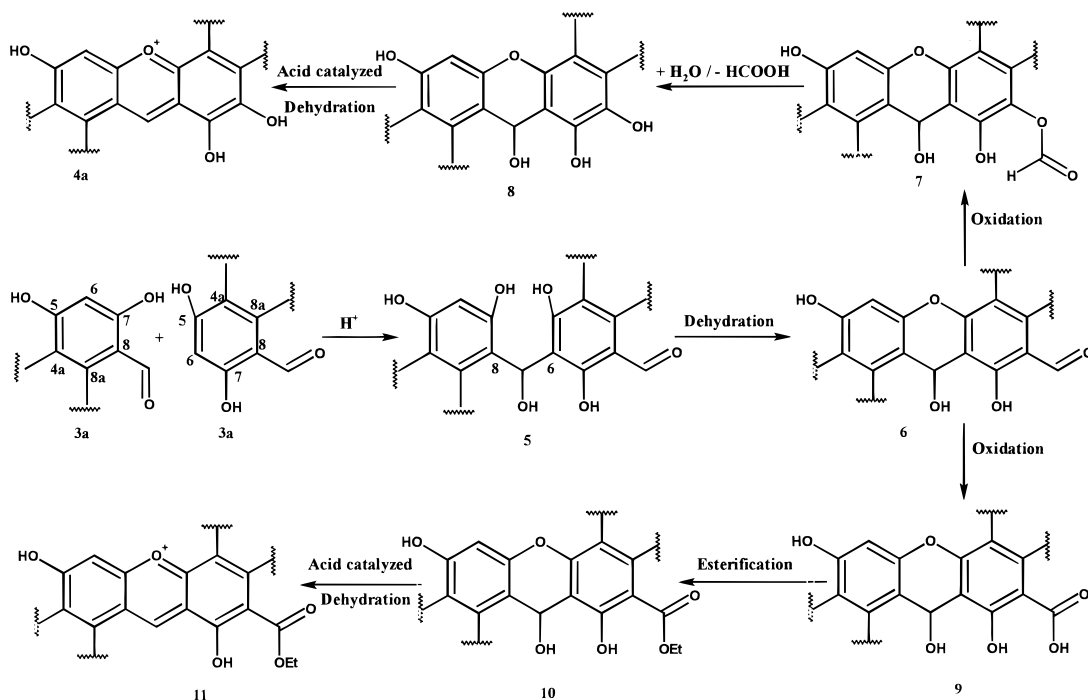


**Figure 10.** Reaction scheme showing the structures and pathways involved in the formation of compounds **4a** and **11** from the **3a** derivative.

usually observed in the region of 400–500 nm during wine aging and confirm their implication in such phenomenon.

The role of these interactions in the color evolution of grape-derived foods may be increased by the involvement of other polyphenolic compounds. In particular, proanthocyanidins, which are the main grape flavanol constituents, could also be involved in such reactions, giving xanthylum salt derivatives. This may increase the importance of such reactions in the color evolution of grape-derived foods.

#### ACKNOWLEDGMENT

We thank Mr. Raymond Baume for discussion on the reactions described in this paper.

#### LITERATURE CITED

- Cheyrier, V.; Rigaud, J.; Souquet, J. M.; Barillère, J. M.; Moutounet, M. Effect of pomace contact and hyperoxidation on the phenolic composition and quality of Grenache and Chardonnay wines. *Am. J. Enol. Vitic.* **1989**, *40*, 36–42.
- Cheyrier, V.; Rigaud, J.; Souquet, J. M.; Duprat, F.; Moutounet, M. Must browning in relation to the behaviour of phenolic compounds during oxidation. *Am. J. Enol.* **1990a**, *41*, 346–349.
- Cheyrier, V.; Rigaud, J.; Moutounet, M. HPLC determination of the free *o*-quinones of trans-caffeoyltartaric acid, 2-*S*-glutathionyl caffeoyltartaric acid and catechin in grape must. *J. Chromatogr.* **1990b**, *472*, 428–432.
- Cheyrier, V.; Fulcrand, H.; Guyot, S.; Oszmianski, J.; Moutounet, M. Reactions of enzymically generated quinones in relation to browning in grape musts and wines. In *Enzymatic Browning and Its Prevention in Foods*; Lee, C. Y., Whitaker, J. R., Eds.; ACS Symposium Series 600; American Chemical Society: Washington, DC, 1995; pp 130–143.
- Cillier, J. J. L.; Singleton, V. L. Nonenzymatic autooxidative phenolic browning reactions in a caffeic acid model system. *J. Agric. Food Chem.* **1989**, *37*, 890–896.
- Dangles, D.; Brouillard, R. UV-visible spectroscopic investigation of the 1,3,6,8-tetrahydroxyxanthylum ion in aqueous solution: structural transformations and molecular complexation with cyclodextrins and caffeine. *New J. Chem.* **1994**, *18*, 287–296.
- Es-Safi, N.; Le Guernevé, C.; Fulcrand, H.; Cheyrier, V.; Moutounet, M. Xanthylum salts involved in wine color evolution. *Int. J. Food Sci. Technol.* **2000a**, *35*, 63–74.
- Es-Safi, N.; Le Guernevé, C.; Cheyrier, V.; Moutounet, M. New polyphenolic compounds obtained by evolution of (+)-catechin and glyoxylic acid in hydro-alcoholic medium. *Tetrahedron Lett.* **2000b**, *41*, 1917–1921.
- Es-Safi, N.; Le Guernevé, C.; Labarbe, B.; Fulcrand, H.; Cheyrier, V.; Moutounet, M. Structure of a new xanthylum derivative. *Tetrahedron Lett.* **1999a**, *40*, 5869–5872.
- Es-Safi, N.; Le Guernevé, C.; Fulcrand, H.; Cheyrier, V.; Moutounet, M. New polyphenolic compounds with xanthylum skeletons formed through reaction between (+)-catechin and glyoxylic acid. *J. Agric. Food Chem.* **1999b**, *47*, 5211–5217.
- Es-Safi, N.; Le Guernevé, C.; Labarbe, B.; Fulcrand, H.; Cheyrier, V.; Moutounet, M. Identification of new xanthylum compounds formed through interaction between (+)-catechin and glyoxylic acid. In *Polyphenol, Wine and Health Communications*; Chèze, C., Vercauteren, J., Eds.; Groupe Polyphenols and the Phytochemical Society of Europe: Bordeaux, France, 1999c; pp 31–32.
- Es-Safi, N.; Le Guernevé, C.; Labarbe, B.; Fulcrand, H.; Cheyrier, V.; Moutounet, M. Characterization of new yellowish compounds which may contribute to colour change in grape derived foods. In *Actualités Oenologiques 1999, 6th International Enology Symposium*; Office International de la Vigne et du vin: Bordeaux, France, June 1999d; pp 548–550.
- Fulcrand, H.; Cheyrier, V.; Oszmianski, J.; Moutounet, M. An oxidized tartaric acid residue as a new bridge potentially competing with acetaldehyde in flavan-3-ol condensation. *Phytochemistry* **1997**, *46*, 223–227.
- Gunata, Z. Y.; Sapis, J. C.; Moutounet, M. Substrates and carboxylic acid inhibitors of grape polyphenoloxidases. *Phytochemistry* **1987**, *26*, 1573–1575.
- Guyot, S.; Vercauteren, J.; Cheyrier, V. Colourless and yellow dimers resulting from (+)-catechin oxidative coupling catalysed by grape polyphenoloxidase. *Phytochemistry* **1996**, *42*, 1279–1288.
- Haslam, E. In vini veritas: oligomeric procyanidins and the aging of red wines. *Phytochemistry* **1980**, *19*, 2577–2582.
- Hrazdina, G.; Borzell, A. J. Xanthylum derivatives in grape extracts. *Phytochemistry* **1971**, *10*, 2211–2213.
- Jurd, L.; Horowitz, R. M. Spectral studies on flavanols—The structure of azelein. *J. Org. Chem.* **1957**, *22*, 1618–1622.
- Jurd, L. In *The Chemistry of Flavonoid Compounds*; Geissman, T. A., Ed.; Pergamon Press: Oxford, U.K., 1962; pp 107–155.
- Jurd, L.; Somers, T. C. The formation of xanthylum salts from proanthocyanidins. *Phytochemistry* **1970**, *9*, 419–427.
- Mabry, T. J.; Markham, K. R.; Thomas, M. B. *The Systematic Identification of Flavonoids*; Springer-Verlag: New York, 1970.
- Oszmianski, J.; Cheyrier, V.; Moutounet, M. Iron-catalyzed oxidation of (+)-catechin in model systems. *J. Agric. Food Chem.* **1996**, *44*, 1712–1715.
- Pierpoint, W. S. The enzymic oxidation of chlorogenic acid and some reactions of the quinones produced. *Biochem. J.* **1966**, *98*, 567–579.
- Simpson, R. F. Factors affecting oxidative browning of white wine. *Vitis* **1982**, *21*, 233–239.
- Rigaud, J.; Cheyrier, V.; Souquet, J. M.; Moutounet, M. Influence of must composition on phenolic oxidation kinetics. *J. Sci. Food Agric.* **1991**, *57*, 55–63.
- Singleton, V. L.; Salgues, M.; Zaya, J.; Trousdale, E. Caftaric acid disappearance and conversion to products of enzymic oxidation in grape must and wine. *Am. J. Enol. Vitic.* **1985**, *36*, 50–56.
- Singleton, V. L. Oxygen with phenols and related reactions in musts, wines, and model systems: observations and practical implications. *Am. J. Enol. Vitic.* **1987**, *38*, 69–76.
- Somers, T. C. The polymeric nature of red pigments. *Phytochemistry* **1971**, *10*, 2175–2186.
- Timberlake, C. F.; Bridle, P. Interactions between anthocyanins phenolic compounds and acetaldehyde. *Am. J. Enol. Vitic.* **1976**, *27* (3), 97–105.

Received for review March 2, 2000. Revised manuscript received June 15, 2000. Accepted June 16, 2000.

JF000283E